

Orbital-spin-phonon coupling in Jahn-Teller-distorted LaMnO_3 : Softening of the 490 and 610 cm^{-1} Raman-active modes

Jiasi Xu, Jung H. Park, and Hyun M. Jang*

Department of Materials Science and Engineering, and Pohang Accelerator Laboratory (PAL), Pohang University of Science and Technology (POSTECH), Pohang 790-784, Republic of Korea

(Received 21 August 2006; revised manuscript received 2 November 2006; published 24 January 2007)

The spin-phonon coupling model that excludes a possible orbital-spin-phonon (OSP) coupling does not adequately explain the softening behavior of the two most intense Raman bands of LaMnO_3 , the parent compound of “colossal” magnetoresistivity. To quantitatively interpret the softening behavior of these two Raman bands at 490 and 610 cm^{-1} , we have derived theoretical expressions for the phonon softening ($\Delta\omega_N$) that take account of a simultaneous OSP coupling. The present analysis successfully explains the softening behavior of these two Raman modes and indicates that a simultaneous OSP coupling is present below the Néel temperature, T_N . The estimated effective force constant (k_{osp}) of the OSP coupling is approximately 70 dynes/cm, which is an order of magnitude smaller than that of the spin-phonon coupling (k_{s-ph}).

DOI: 10.1103/PhysRevB.75.012409

PACS number(s): 75.10.-b, 75.50.Ee, 63.20.Kr, 78.30.-j

Divalent cation-modified lanthanum manganites (LaMnO_3 ; LMO) that display “colossal” magnetoresistivity have rekindled our interests in these strongly correlated electronic oxides. The subtle interplay between spin, charge, orbital, and lattice degrees of freedom is the most prominent feature in this class of perovskites and is believed to be the key to understanding their extraordinary transport and magnetic properties.¹⁻⁴ The study of the parent compound LMO is a useful starting point to a consistent understanding of this complex interplay between various degrees of freedom.

In the perovskite orthorhombic LMO (space group $Pnma$), all of the Mn ions are trivalent with four electrons in 3d orbitals. Among these four electrons, one electron occupies one of the doubly degenerate e_g orbitals, and thus the ion has both spin and orbital degrees of freedom.^{5,6} Below 780 K, the orbital degree of freedom is spontaneously frozen by the real-space C-type ordering of the e_g orbitals accompanied by a Jahn-Teller-type lattice distortion of the MnO_6 octahedra.^{6,7} In addition, the spin ordering appears below $T_N \approx 140$ K, where spins, due to the Hund’s exchange coupling,⁶ are aligned ferromagnetically in the basal plane and antiferromagnetically along the perpendicular direction (A-type antiferromagnetic ordering).

Because the Raman scattering technique is highly sensitive to local symmetry change, this method has been applied to the study of the lattice modulation of spins, orbitals, and electrons (polarons) in manganites.^{8,9} Indeed, Granado *et al.*^{10,11} obtained an evidence of the spin-phonon coupling by analyzing the softening of the Raman active 610 cm^{-1} and 490 cm^{-1} modes of LMO below T_N . Since the orbital ordering temperature (T_{oo}) of LMO is 780 K, a simultaneous spin-orbital-phonon coupling is expected below T_N (140 K). In spite of this expectation, little progress has been made along this line. Here we report an interesting indication of a simultaneous coupling of orbital, spin, and lattice degrees of freedom by carefully examining the softening behavior of Raman active phonons.

Orthorhombic LMO ($Pnma$) polycrystalline samples used in the present Raman and magnetization measurements were

prepared by a conventional solid-state reaction method, similar to the method employed by Oseroff *et al.*¹² The calcined power (1200 °C for 24 h) was pressed into pellets and sintered at 1300 °C for 24 h, followed by slow cooling to room temperature with a cooling rate of 100 °C/h. To maintain the oxygen content of sintered LMO pellet at its stoichiometric value (i.e., 3.0), a post annealing was performed at 900 °C for 24 h in N_2 flow, using Ti metal as a getter.¹³ Figure 1(a) shows the temperature dependence of the normalized sublattice magnetization of LMO measured using a SQUID magnetometer (Quantum Design MPMS-5S). The $M(T)$ result indicates that the present LMO is not strictly antiferromagnetic but is weakly ferromagnetic¹⁰ presumably due to canted spin structure. Thus, the measurement only reflects $M(T)$ under the assumption that this small canting of the spin moments is not temperature dependent. A close similarity between our $M(T)$ curve at 100 Oe and the $M(T)$ curve obtained from the neutron diffraction measurements (stoichiometric $\text{LaMnO}_{3.0}$ sample-IIa of Ref. 13) indicates that this assumption seems to be valid.

The Raman measurements were performed using a NRS-2100 triple-grating spectrometer (JASCO, Japan) equipped with a cryogenic temperature controller (ST-100 Cryostat System) and a Coherent Innova 90C Ar⁺-laser operating at 514.5 nm. The Raman scattering was done using 180° back-scattering geometry in the temperature range between 5 and 300 K. In order to avoid heating of the sample, the incident laser power was kept below 15 mW focused in a diameter of ~ 50 μm . To minimize surface decomposition effects, all the spectra were taken on fresh broken surfaces, exposed to the air for a few minutes before being measured.¹⁰

In the orthorhombic LMO with $Pnma$ symmetry, the two most intense bands that appear at 490 and 610 cm^{-1} undergo a softening below T_N .¹⁰ By considering the nearest neighbors of the Mn^{3+} ion and using the molecular field approximation,¹¹ one can show that the frequency modulation due to a spin-phonon interaction is directly proportional to the square of $M(T)$, as manifested in Eq. (1)

$$(\Delta\omega_\alpha)_{s-ph} \approx -\frac{2}{\mu_\alpha\omega_0} \left\{ \frac{\partial^2 J_{xz}}{\partial u_{o1}^2} - \frac{1}{2} \frac{\partial^2 J_y}{\partial u_{o2}^2} \right\} \left[\frac{M(T)}{4\mu_B} \right]^2, \quad (1)$$

where $\langle S_i S_j \rangle_{xz} = -\langle S_i S_j \rangle_y \approx +4\{M(T)/4\mu_B\}^2$, and $M(T)$ is the FM sublattice magnetization per Mn^{3+} . O(1) refers to the equatorial O^{2-} ions whereas O(2) denotes the apical ones in a MnO_6 octahedron. The second partial derivative of the exchange constant (J_{xz} or J_y) appeared in Eq. (1) represents a phonon modulation of the superexchange integral, i.e., spin-phonon coupling. According to Eq. (1), a plot of $\ln\{\omega_\alpha(T_N) - \omega_\alpha(T)\}$ as a function of $\ln\{M(T)/4\mu_B\}$ should yield a linear line with the slope being +2 if the spin-phonon coupling is solely responsible for the Raman frequency softening below T_N . The logarithmic plot has been made using the $M(T)$ data [Fig. 1(a)] at 100 Oe and Raman mode frequency (filled circles in Fig. 2). As shown in Fig. 1(b), the plot is approximately characterized by a linear line only for a limited temperature range substantially below T_N ($T \leq 90$ K for 610 cm^{-1} , and $T \leq 110$ K for 490 cm^{-1} mode). Furthermore, the estimated slope (S) is substantially different from the theoretical value of +2, indicating that the spin-phonon coupling alone does not adequately describe the observed softening below T_N .

Considering that the orbital ordering is intimately related to the Jahn-Teller distortion,^{6,14} one can partly attribute the observed phonon softening to a simultaneous orbital-spin-phonon (OSP) coupling. Indeed, Murakami *et al.*⁷ presented a direct evidence of the orbital ordering in LaMnO_3 by monitoring the (3,0,0) reflection intensity of resonant x-ray scattering. Their study shows that the order parameter of the orbital ordering starts to increase at a certain onset temperature (~ 300 K) well above T_N and remains nearly constant below T_N , suggesting that the spin and orbital degrees of freedom are coupled.⁷ To assess the validity of the OSP coupling, we have theoretically examined the softening behavior of these two phonons using the experimental Raman and $M(T)$ data.

In the work of Raman spectroscopic study of the cooperative Jahn-Teller distortion in LMO,¹⁵ the frequency decrease with a concomitant peak broadening at a higher temperature region ($T=200-700$ K) was attributed to the effect of anharmonic phonon scattering.¹⁶ In fact, a continuous increase in the linewidth with temperature¹⁵ suggests that this effect also works for $T < T_N$, but accompanied by other effects that relate to the spin ordering below T_N . Therefore, for quantitative analysis, the exact degree of the frequency softening due to the spin ordering must be safely separated from the frequency change caused by the anharmonic scattering. A simplified approximation to the anharmonic phonon scattering [16] leads to the formula: $\omega(T) = \omega_0 - C(1 + \frac{2}{e^x - 1})$, where $x = \hbar\omega/2k_B T$. The low-temperature (low- T) Raman shift, if there were no spin ordering, would be simulated by first fitting this equation to the high- T part to find ω_0 and C and then applying these parameters to the low- T range. The fitting produces $\omega_0 = 509.5 \text{ cm}^{-1}$, $C = 10.63 \text{ cm}^{-1}$ for the 490 cm^{-1} mode, and $\omega_0 = 614.7 \text{ cm}^{-1}$, $C = 2.4 \text{ cm}^{-1}$ for the 610 cm^{-1} mode. The experimental frequency and the simulated Raman shift are presented in Fig. 2 by filled and open

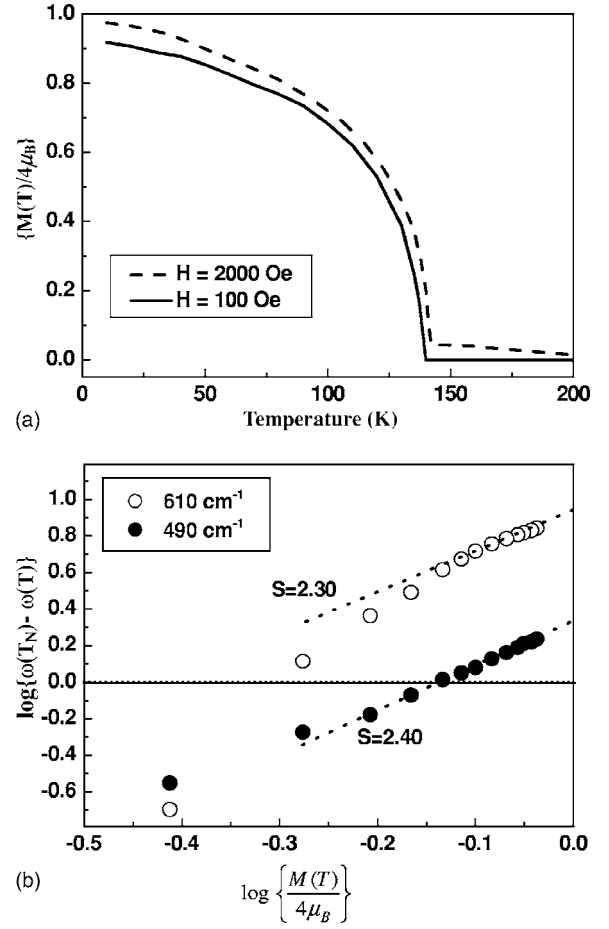


FIG. 1. (a) Temperature-dependent sublattice magnetization of orthorhombic LaMnO_3 at two different magnetic fields. (b) A logarithmic plot of the mode frequency softening $\{\omega_\alpha(T_N) - \omega_\alpha(T)\}$ with respect to the sublattice magnetization for temperatures between 10 and 140 K.

circles, respectively. Since the parameter “ C ” is a measure of the strength of phonon coupling, our estimated result reflects the fact that the 490 cm^{-1} phonon corresponds to the cooperative Jahn-Teller mode.¹⁵

To proceed further, we now define $\Delta\omega_N(T)$ as the discrepancy between the experimental phonon frequency (ω_{exp}) and the natural extension from the high- T part (ω'_{ext}). For $T < T_N$, $\omega_{exp} = \omega_{int} + \Delta\omega_{s-ph} + \Delta\omega_{orb-ph} + \Delta\omega_{osp} + \Delta\omega_{anh}$. On the other hand, $\omega'_{ext} = \omega_{int} + \Delta\omega_{orb-ph} + \Delta\omega_{anh}$, where ω_{int} is the intrinsic phonon frequency. Thus, $\Delta\omega_N$ can be simplified as

$$\Delta\omega_N \equiv \omega_{exp} - \omega'_{ext} = \Delta\omega_{s-ph} + \Delta\omega_{osp} \leq 0. \quad (2)$$

Our next task is to correlate $\Delta\omega_N$ with the correlation function of relevant order parameters. To do this, we have considered a suitable Hamiltonian. In the Jahn-Teller-distorted magnetic materials, the Hamiltonian that takes account of both the spin-phonon coupling and the orbital-spin-phonon (OSP) coupling can be written as

$$H = - \sum_{i,j} (J_1 S_i S_j + 4J_3 S_i S_j \tau_i \tau_j), \quad (3)$$

where $\tau_i \tau_j$ is the orbital correlation operator.^{5,17} Considering the modulation of the phonon frequency ($\Delta\omega$) due to the

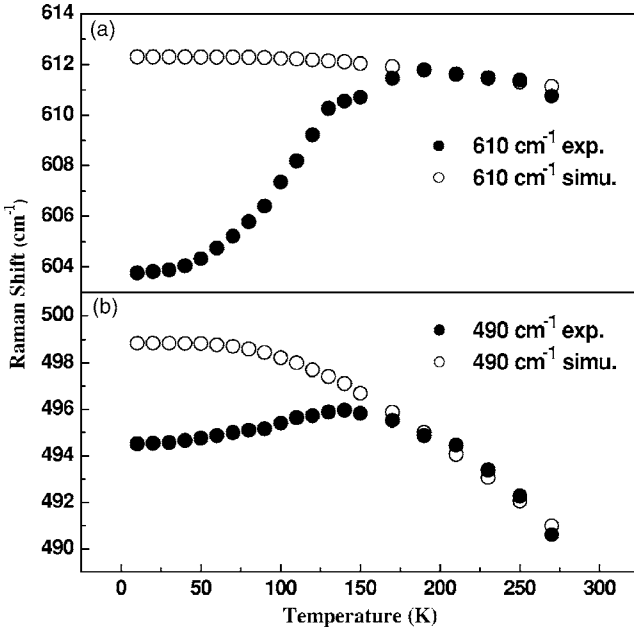


FIG. 2. Comparison of the experimental Raman shift (filled circles) with the simulated one produced from the anharmonic phonon-scattering model for (a) 610 cm^{-1} and (b) 490 cm^{-1} modes.

coupling of phonons¹⁸ to other ordering parameters, one can readily establish the following expression from Eq. (3):

$$\Delta\omega_N(T) = -\frac{1}{2\mu\omega_0} \sum_{i,j} \left(\frac{\partial^2 J_1}{\partial u^2} S_i S_j + 4 \frac{\partial^2 J_3}{\partial u^2} S_i S_j \tau_i \tau_j \right). \quad (4)$$

The first term in the bracket of Eq. (4) represents the effective force constant of spin-phonon coupling (k_{s-ph}), whereas the second term corresponds to the effective force constant of OSP coupling (k_{osp}). Using the multivariable Taylor expansion, one can show that

$$\sum_{i,j} (S_i S_j) (\tau_i \tau_j) \approx \sum_{i,j} \{ \langle S_i S_j \rangle \langle \tau_i \tau_j \rangle + \langle S_i S_j \rangle \delta\tau + \langle \tau_i \tau_j \rangle \delta S \}, \quad (5)$$

where

$$\delta\tau \equiv \tau_i \tau_j - \langle \tau_i \tau_j \rangle \Big|_{S_i S_j = \langle S_i S_j \rangle} \quad \text{and} \quad \delta S \equiv S_i S_j - \langle S_i S_j \rangle \Big|_{\tau_i \tau_j = \langle \tau_i \tau_j \rangle}. \quad (6)$$

The bracket notation refers to the ensemble average if there were no coupling between orbital and spin degrees of freedom. Using Eqs. (4)–(6), one can eventually establish the following relation for the in-phase stretching 610 cm^{-1} mode:

$$\begin{aligned} \Delta\omega_N^{610}(T)(-\omega_0) \left(\frac{m}{2} \right) &= \left[\frac{\partial^2 J_1^{xz}}{\partial u_{O1}^2} + 4 \frac{\partial^2 J_3^{xz}}{\partial u_{O1}^2} (\langle \tau_i \tau_j \rangle_{xz} + \delta\tau_{xz}) \right] \\ &\times \left(\frac{M(T)}{4\mu_B} \right)^2 + 4 \frac{\partial^2 J_3^{xz}}{\partial u_{O1}^2} \\ &\times \langle \tau_i \tau_j \rangle_{xz} \delta S_{xz}. \end{aligned} \quad (7)$$

In the out-of-phase bending at 490 cm^{-1} [$A_g(3)$ symmetry], both equatorial O(1) and apical O(2) are involved and

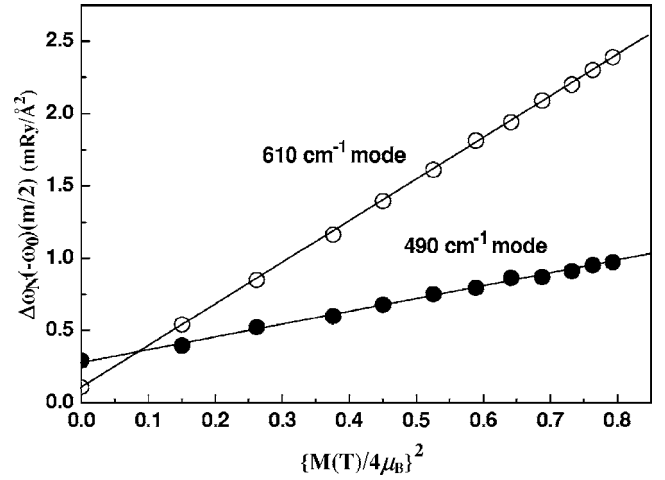


FIG. 3. Linear fitting of $\Delta\omega_N(-\omega_0)(m/2)$ with $\{M(T)/4\mu_B\}^2$ for both 610 cm^{-1} (open circles) and 490 cm^{-1} (filled circles) modes, showing nonzero values of the intercept (B). Here Ry denotes the Rydberg constant and is equivalent to 2.1799×10^{-18} J.

vibrate normal to their Mn-O bonds.¹⁹ For a pure LMO, we further have $\langle \tau_i \tau_j \rangle_y = -\langle \tau_i \tau_j \rangle_{xz}$ and $\langle S_i S_j \rangle_y = -\langle S_i S_j \rangle_{xz}$, thus $\delta S_y = -\delta S_{xz}$, and $\delta\tau_y = -\delta\tau_{xz}$. Replacing the mass of oxygen (m) by its effective mass (m/γ) for a bending mode,²⁰ we obtained the following expression:

$$\begin{aligned} \Delta\omega_N^{490}(T)(-\omega_0) \left(\frac{m}{2} \right) &= \gamma \left[\frac{\partial^2 J_1^{xz}}{\partial u_{O1}^2} - \frac{1}{2} \frac{\partial^2 J_1^y}{\partial u_{O2}^2} + 4 \left(\frac{\partial^2 J_3^{xz}}{\partial u_{O1}^2} \right. \right. \\ &\quad \left. \left. + \frac{1}{2} \frac{\partial^2 J_3^y}{\partial u_{O2}^2} \right) (\langle \tau_i \tau_j \rangle_{xz} + \delta\tau_{xz}) \right] \left(\frac{M(T)}{4\mu_B} \right)^2 \\ &\quad + 4\gamma \left(\frac{\partial^2 J_3^{xz}}{\partial u_{O1}^2} + \frac{1}{2} \frac{\partial^2 J_3^y}{\partial u_{O2}^2} \right) \langle \tau_i \tau_j \rangle_{xz} \delta S_{xz}. \end{aligned} \quad (8)$$

Equations (7) and (8) have a common form of “ $Y=AX+B$ ” with Y corresponding to the left-hand side of the equation containing $\Delta\omega_N$ and X corresponding to the square of the sublattice magnetization. Because $\langle \tau_i \tau_j \rangle$ is obviously nonzero below T_{oo} and δS is nonzero only in the case of spin-orbital coupling [Eq. (6)], the intercept (B) is nonzero only if a simultaneous OSP coupling is present. As can be deduced from Eqs. (4), (7), and (8), the term B can be interpreted as the effective force constant of the OSP coupling (k_{osp}). k_{osp} , as estimated from the intercept, is approximately 70 dynes/cm for the 490 cm^{-1} bending mode. On the other hand, if the OSP coupling were absent, the slope A would represent $(1/4)k_{s-ph}$. The force constant of the spin-phonon coupling alone (k_{s-ph}), as estimated from the slope, is ~ 1000 dynes/cm for the 490 cm^{-1} mode, which is an order of magnitude larger than k_{osp} .

As shown in Fig. 3, there is a good linear correlation between $\Delta\omega_N(T)$ and $\{M(T)/4\mu_B\}^2$, which is in accordance with the theoretical prediction [Eqs. (7) and (8)]. $\Delta\omega_N(T)$ value for the two distinct modes were estimated using the results shown in Fig. 2. As shown in Fig. 3, a finite positive

value of the intercept is evident for both modes. This clearly indicates that the spin ordering and the orbital ordering are not independent but are coupled to each other through a phonon modulation of the superexchange integral ($\partial^2 J / \partial u^2$) for temperatures below T_N . The nonzero intercept also suggests that the degree of the orbital-spin coupling does not vanish completely at T_N but remains nonzero for a finite temperature range above T_N .⁷ A slightly higher value of B for the 490 cm^{-1} mode than that for 610 cm^{-1} indicates an important role of the apical O(2) vibration in the phonon modulation of the superexchange interaction [i.e., $\partial^2 J_3 / \partial u_{O2}^2$, appeared in the intercept B of Eq. (8)].

In conclusion, an interesting indication of the OSP cou-

pling in Jahn-Teller-distorted LMO was obtained by theoretically analyzing the softening behavior of the two intense Raman bands. The OSP coupling is effective below the spin ordering temperature, which contributes to the phonon softening below T_N . However, the present analysis should be supported by more concrete experimental evidences before one can come to the conclusion that the OSP coupling clearly exists below T_N .

We express our gratitude to B. I. Min at the Physics Dept. of POSTECH, Korea for useful discussion. This work was supported by the Korea Science and Engineering Foundation (KOSEF) under Contract No. R01-2005-000-10354-0.

*Author to whom correspondence should be addressed. Email address: hmjang@postech.ac.kr

¹W. Archibald, J.-S. Zhou, and J. B. Goodenough, *Phys. Rev. B* **53**, 14445 (1995).

²A. J. Millis, *Phys. Rev. B* **53**, 8434 (1996).

³S. Mori, C. H. Chen, and S.-W. Cheong, *Nature (London)* **392**, 473 (1998).

⁴S. Yunoki, A. Moreo, and E. Dagotto, *Phys. Rev. Lett.* **81**, 5612 (1998); J. van den Brink, G. Khaliullin, and D. Khomskii, *ibid.* **83**, 5118 (1999); T. Hotta, Y. Takada, H. Koizumi, and E. Dagotto, *ibid.* **84**, 2477 (2000).

⁵K. I. Kugel' and D. I. Khomskii, *Sov. Phys. Usp.* **25**, 231 (1982).

⁶D. I. Khomskii and G. A. Sawatzky, *Solid State Commun.* **102**, 87 (1997).

⁷Y. Murakami, J. P. Hill, D. Gibbs, M. Blume, I. Koyama, M. Tanaka, H. Kawata, T. Arima, Y. Tokura, K. Hirota, and Y. Endoh, *Phys. Rev. Lett.* **81**, 582 (1998).

⁸E. Saitoh, S. Okamoto, K. T. Takahashi, K. Tobe, K. Yamamoto, T. Kimura, S. Ishihara, S. Maekawa, and Y. Tokura, *Nature (London)* **410**, 180 (2001).

⁹V. B. Podobedov, A. Weber, D. B. Romero, J. P. Rice, and H. D. Drew, *Phys. Rev. B* **58**, 43 (1998).

¹⁰E. Granado, N. O. Moreno, A. Garcia, J. A. Sanjurjo, C. Rettori, I. Torriani, S. B. Oseroff, J. J. Neumeier, K. J. McClellan, S.-W.

Cheong, and Y. Tokura, *Phys. Rev. B* **58**, 11435 (1998).

¹¹E. Granado, A. Garcia, J. A. Sanjurjo, C. Rettori, I. Torriani, F. Prado, R. Sánchez, A. Caneiro, and S. B. Oseroff, *Phys. Rev. B* **60**, 11879 (1999).

¹²S. B. Oseroff, M. Torikachvili, J. Singley, S. Ali, S. W. Cheong, and S. Schultz, *Phys. Rev. B* **53**, 6521 (1996).

¹³Q. Huang, A. Santoro, J. W. Lynn, R. W. Erwin, J. A. Borchers, J. L. Peng, and R. L. Greene, *Phys. Rev. B* **55**, 14987 (1997).

¹⁴E. Granado, J. A. Sanjurjo, C. Rettori, J. J. Neumeier, and S. B. Oseroff, *Phys. Rev. B* **62**, 11304 (2000).

¹⁵L. Martín-Carrón and A. de Andrés, *Eur. Phys. J. B* **22**, 11 (2001).

¹⁶M. Balkanski, R. F. Wallis, and E. Haro, *Phys. Rev. B* **28**, 1928 (1983).

¹⁷M. D. Kaplan and B. G. Vekhter, *Cooperative Phenomena in Jahn-Teller Crystals* (Plenum Press, New York, 1995), Chap. 4.

¹⁸W. Baltensperger and J. S. Helman, *Helv. Phys. Acta* **41**, 668 (1968).

¹⁹M. N. Iliev, M. V. Abrashev, H. G. Lee, V. N. Popov, Y. Y. Sun, C. Thomsen, R. L. Meng, and C. W. Chu, *Phys. Rev. B* **57**, 2872 (1998).

²⁰ γ is a factor that describes the effective mass μ in a spring system where the mass vibrates perpendicular to the spring axis with $\mu = m / \gamma$. It can be readily shown that $\gamma \leq 1$.